

Properties of S waves near a kiss singularity: a comparison of exact and ray solutions

Václav Vavryčuk

Geophysical Institute, Academy of Sciences of the Czech Republic, Boční II/1401, 141 31 Praha 4, Czech Republic. E-mail: vv@ig.cas.cz

Accepted 1999 March 26. Received 1999 March 16; in original form 1998 August 21

SUMMARY

We have studied the properties of S waves generated by a point source in a homogeneous, transversely isotropic, elastic medium, propagating in directions close to that of a kiss singularity, which coincides with the symmetry axis of the medium. We have proved analytically as well as numerically that the ray solution can describe the S waves correctly far from the source in all directions, including that of the kiss singularity. We have found that, in contrast to the far-field P wave, which can be reproduced satisfactorily by the zeroth-order ray approximation in all directions from the source, the far-field S waves can be reproduced satisfactorily by the zeroth-order ray approximation only in directions far from the kiss singularity. In directions near the kiss singularity, the first-order ray approximation must also be considered, because the zeroth-order ray approximation yields distorted results. The first-order ray approximation can be of high frequency and can be detected in the far field.

Key words: anisotropy, Green's function, kiss singularity, ray theory, S waves.

1 INTRODUCTION

S -wave singularities are very important when S waves are being modelled in anisotropic media. They are defined as the directions where two S waves have coincident phase velocities, and are very common in all types of anisotropy. In directions near singularities, the polarization of plane S waves can change very rapidly, and the amplitude and polarization of S waves with curved wavefronts can behave quite anomalously (Crampin & Yedlin 1981). We distinguish between kiss, point and line singularities (Crampin 1991); of these, the point singularity (also called the 'conical point') affects the geometry of the rays and wavefield in the most complicated and profound way. It is known that zeroth-order ray theory is inapplicable to modelling of the wavefield near the point singularity, and thus other techniques such as the Radon transform (Wang & Achenbach 1994), reflectivity (Crampin 1991) or Maslov method (Rümpker & Thomson 1994) must be used. It is not clear, however, how much the wavefield is affected by a kiss singularity. This singularity is defined as the direction in which two S -wave phase-velocity sheets touch *tangentially* at an isolated point. Since the group velocities near the kiss singularity behave quite regularly, it is believed that 'the waveforms of initial shear-wave pulse will propagate with little distortion' and 'the shear waves will split in a regular manner without any particular anomaly' (Crampin 1991). This implies that ray theory (Červený 1972; Červený *et al.* 1977) could be used to model the wavefield near the kiss singularity.

In this paper we shall focus on modelling S waves using ray theory when the S waves propagate close to a kiss singularity. We shall study S waves generated by a point source situated in a homogeneous, transversely isotropic medium (hereafter TI medium). In TI media, the kiss singularity coincides with the symmetry axis. If we assume a vertical symmetry axis, the split S waves become the SV and SH waves, with polarization vectors near the singularity as shown in Fig. 1. We shall consider only TI media with no triplications on the SV or SH wavefronts, and compare exact and ray solutions of S waves in the far field. We shall show that zeroth-order ray theory

Polarization vectors near a kiss singularity

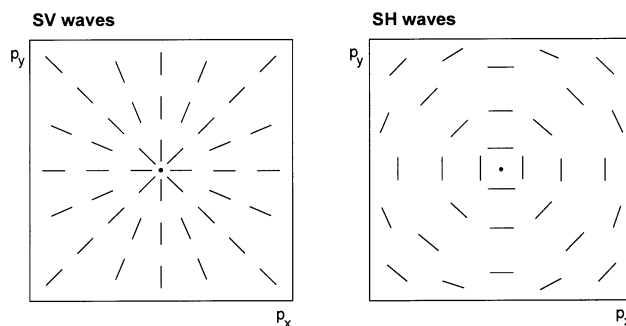


Figure 1. Horizontal projections of polarization vectors of the SV and SH waves near a kiss singularity in the p_x - p_y plane, where p_x and p_y are the horizontal components of the slowness vector.

yields distorted results near the kiss singularity. If we consider the first-order ray approximation, calculated by Vavryčuk & Yomogida (1996) and by Vavryčuk (1997), however, we obtain a satisfactory result. The first-order ray approximation has a simple analytical form and its properties will be discussed in detail.

2 THEORY

2.1 Exact integral solution of the Green tensor

The exact elastodynamic Green tensor $G_{kl}(\mathbf{x}, t)$ for unbounded, homogeneous, anisotropic, elastic media can be expressed as follows (Burridge 1967, eq. 4.6; Wang & Achenbach 1994, eq. 13):

$$G_{kl}(\mathbf{x}, t) = -\frac{H(t)}{8\pi^2\rho} \sum_{m=1}^3 \int_{S(\mathbf{n})} F_{kl}^m(\mathbf{n}) \dot{\delta}\left(t - \frac{\mathbf{n} \cdot \mathbf{x}}{c^m}\right) dS(\mathbf{n}), \quad (1)$$

where

$$F_{kl}^m(\mathbf{n}) = \frac{g_k^m g_l^m}{(c^m)^3}.$$

The superscript $m = 1, 2, 3$ denotes the type of wave (P , $S1$ or $S2$), $\mathbf{g} = \mathbf{g}(\mathbf{n})$ denotes the unit polarization vector, $c = c(\mathbf{n})$ is the phase velocity, ρ is the density of the medium, t is time, $H(t)$ is the Heaviside step function, $\dot{\delta}(t)$ is the time derivative of the Dirac delta function, \mathbf{x} is the position vector of the observation point, and \mathbf{n} is the phase normal. The integration is over the unit sphere $S(\mathbf{n})$. Formula (1) represents the exact solution for homogeneous, weakly as well as strongly, anisotropic media, containing far-field as well as near-field waves, and is valid at all distances and in all directions, including the S -wave singularities. For an *isotropic medium*, integral (1) can be evaluated analytically to yield the well-known Stokes solution (see Mura 1991; pp. 61–63). For a *transversely isotropic medium*, integral (1) has also been evaluated analytically, but only for the symmetry axis direction (Payton 1977, 1983). For other directions, the integral should be evaluated either numerically, or it should be expanded asymptotically.

2.2 Far-field approximation versus the zeroth-order ray approximation

On evaluating eq. (1) by the stationary phase method, we obtain the far-field approximation of the Green tensor in the following form (Kendall *et al.* 1992; eq. 1):

$$G_{kl}^{\text{far}}(\mathbf{x}, t) = \frac{1}{4\pi\rho} \sum_{m=1}^3 \frac{1}{v^m \sqrt{K_p^m}} \frac{g_k^m g_l^m}{r} \delta(t - \tau^m(\mathbf{x})), \quad (2)$$

where the superscript m denotes the type of wave, v is the group velocity, \mathbf{g} is the unit polarization vector, r is the distance of the observation point from the source, $\delta(t)$ is the Dirac delta function, τ is the travelttime, and K_p is the Gaussian curvature of the slowness surface. The slowness surface is assumed to be convex in all directions, and hence no parabolic points are considered and the Gaussian curvature is always positive. Formula (2) is valid for all directions from the source, except those in the close vicinity of a singularity. In the

singularity, the asymptotic calculation of (1) requires special treatment, because the integrand's amplitude $F_{kl}(\mathbf{n})$ in (1) is not continuous, and the standard method of stationary phase cannot be applied. At a point singularity, integral (1) has been calculated asymptotically by Buchwald (1959), Lighthill (1960) and Burridge (1967). The asymptotic formula at the kiss singularity, however, is not mentioned in the literature, even though the case of the kiss singularity is not as complicated as that of the point singularity. For the asymptotic calculation of (1) at the kiss singularity in TI media, see the Appendix.

Now we are faced with the problem of defining the zeroth-order ray-theory Green tensor $G_{kl}^{(0)}(\mathbf{x}, t)$ in a medium in which a kiss singularity appears. The most common technique is to define the zeroth-order term of the ray series by eq. (2) in directions far from the kiss singularity, and by another formula in directions close to the kiss singularity. From these zeroth-order terms, we can then construct the whole ray series (see Vavryčuk & Yomogida 1996). Thus the waves will be described by two different ray expansions with different and limited regions of applicability. Unfortunately, for directions in between (not close to but also not far from the singularity), we may obtain a gap with no satisfactory ray solution. It is highly desirable, however, to find one ray solution describing the waves in all directions, including the singularity direction. For this purpose, we use a different approach in this paper. We define the zeroth-order ray-theory Green tensor $G_{kl}^{(0)}(\mathbf{x}, t)$ by formula (2) not only in regular directions, but also in directions close to the singularity, or even at the singularity. As a consequence, the zeroth-order ray approximation will differ from the far-field approximation in directions close to the singularity. This inconsistency will be corrected by including higher-order ray approximations. We shall show that it is really possible to obtain a single ray solution that describes the far-field waves correctly in all directions, including that of the kiss singularity.

2.3 The zeroth-order ray-theory Green tensor in the TI medium

Next we assume a homogeneous transversely isotropic medium with a vertical axis of symmetry. In this case, the $S1$ and $S2$ waves become SV and SH waves, and all quantities in eq. (2) can be expressed analytically. For the SH -wave Green tensor, we obtain a simple analytical formula (Vavryčuk & Yomogida 1996; eq. 25). For the P - and SV -wave Green tensors, the formulae are rather cumbersome, because explicit analytical formulae for group velocity v and Gaussian curvature K_p are rather long and complicated. The formulae simplify considerably if we assume that the observation point lies in the direction of the symmetry axis. For the zeroth-order ray-theory Green tensor at the kiss singularity we obtain

$$\begin{aligned} G_{11}^{(0)}(z, t) &= \frac{1}{4\pi\rho} \left[a_{11} - \frac{(a_{13} + a_{44})^2}{a_{33} - a_{44}} \right]^{-1} \frac{1}{|z|} \delta\left(t - \frac{|z|}{\sqrt{a_{44}}}\right), \\ G_{22}^{(0)}(z, t) &= \frac{1}{4\pi\rho} \frac{1}{a_{66}} \frac{1}{|z|} \delta\left(t - \frac{|z|}{\sqrt{a_{44}}}\right), \\ G_{33}^{(0)}(z, t) &= \frac{1}{4\pi\rho} \left[a_{44} + \frac{(a_{13} + a_{44})^2}{a_{33} - a_{44}} \right]^{-1} \frac{1}{|z|} \delta\left(t - \frac{|z|}{\sqrt{a_{33}}}\right), \end{aligned} \quad (3)$$

where we have used the following basis of polarization vectors:

$$\mathbf{g}^P = (0, 0, 1)^T, \quad \mathbf{g}^{SV} = (1, 0, 0)^T, \quad \mathbf{g}^{SH} = (0, -1, 0)^T. \quad (4)$$

Component $G_{33}^{(0)}(z, t)$ describes the *P* wave, and components $G_{11}^{(0)}(z, t)$ and $G_{22}^{(0)}(z, t)$ describe the *S* wave. Other components of the Green tensor are zero.

As expected, formula (3) describes the *P* wave in the far field correctly, but the *S* wave is incorrect. Formula (3) was derived from (2), which is inapplicable to the *S* wave at the singularity. The incorrectness of (3) can be seen by the following.

(1) Since the Gaussian curvatures of the *SV*- and *SH*-wave slowness surfaces in (2) are different at the kiss singularity, $K_p^{SV} \neq K_p^{SH}$, we find that $G_{11}^{(0)}(z, t) \neq G_{22}^{(0)}(z, t)$. Obviously, this is incorrect, because no direction in the *x*-*y* plane is preferential in the propagation of waves along the symmetry axis, and the components of the Green tensor in the far field $G_{11}^{far}(z, t)$ and $G_{22}^{far}(z, t)$ must be equal.

(2) Polarization vectors \mathbf{g}^{SV} and \mathbf{g}^{SH} are non-unique at the singularity. In principle, any two perpendicular vectors lying in the horizontal plane can be used for \mathbf{g}^{SV} and \mathbf{g}^{SH} at the singularity, and must produce the same form of Green tensor in the far field. However, formula (3) depends on the choice of vectors \mathbf{g}^{SV} and \mathbf{g}^{SH} and will be different for vectors other than those specified in (4).

In the next section we show that we can overcome the difficulties of the ray solution by considering the first-order ray approximation.

2.4 The first-order ray-theory Green tensor in the TI medium

The first-order ray approximation of the Green tensor for a homogeneous TI medium consists of several terms (Vavryčuk 1997): the first term is significant near the singularity (hereafter the ‘near-singularity’ term), and the other terms are significant in the near field (hereafter the ‘near-field’ terms). Since we are dealing with waves in the far field, we shall consider only the near-singularity term. This term is composed of additional as well as principal components of the *SV*- and *SH*-wave first-order approximations. It has the following form (Vavryčuk & Yomogida 1996; eq. 28; Vavryčuk 1997; eqs 23a, 24a):

$$G_{kl}^{S(1)}(\mathbf{x}, t) = \frac{1}{4\pi\rho\sqrt{a_{44}}} \frac{g_k^{SH} g_l^{SH} - g_k^{SH\perp} g_l^{SH\perp}}{R^2} \times [H(t - \tau^{SH}) - H(t - \tau^{SV})], \quad (5)$$

where $\mathbf{g}^{SH\perp} = (\cos \varphi, \sin \varphi, 0)^T$ is the unit vector perpendicular to $\mathbf{g}^{SH} = (\sin \varphi, -\cos \varphi, 0)^T$, $R = r \sin \vartheta$ is the distance of the observation point from the singularity direction, r is the distance of the observation point from the source, and ϑ and φ are the standard spherical angles of the \mathbf{x} vector. It follows from eq. (5) that the amplitude of the near-singularity term depends on distance as $1/R^2$. Thus for observation points close to the singularity ($R \rightarrow 0$), this term is prominent (see Fig. 2). It can be prominent not only in the near field but also in the far field, because in the far field ($r \rightarrow \infty$) the distance R can also vanish (for $\vartheta \rightarrow 0$). This is of particular interest, because we usually assume that the higher-order ray approximations are negligible in the far field as compared to the zeroth-order ray approximation.

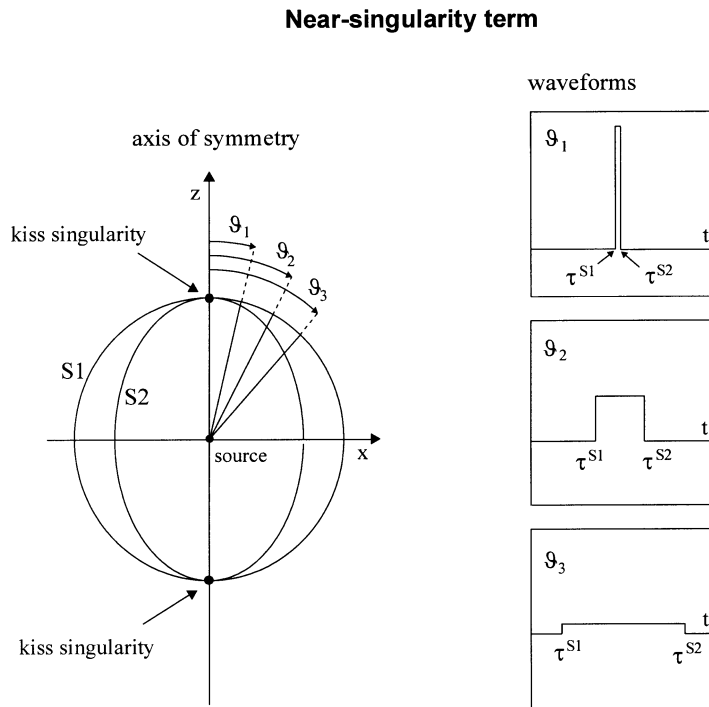


Figure 2. Geometry of *S* wavefronts radiated from a point source in the TI medium (left-hand plot), together with schematically shown waveforms of the near-singularity term for three observation points with rays deviating from the singularity by angles of ϑ_1, ϑ_2 and ϑ_3 (right-hand plots).

At the singularity, eq. (5) yields

$$\begin{aligned}
 G_{11}^{S(1)}(z, t) &= \lim_{g \rightarrow 0} G_{11}^{S(1)}(\mathbf{x}, t) \\
 &= \frac{1}{4\pi\rho\sqrt{a_{44}}} \lim_{g \rightarrow 0} \left[\frac{\tau^{SH} - \tau^{SV}}{r^2 \sin^2 g} \right] \\
 &\quad \times \lim_{g \rightarrow 0} \left[\frac{H(t - \tau^{SV}) - H(t - \tau^{SH})}{\tau^{SH} - \tau^{SV}} \right] \\
 &= \frac{1}{8\pi\rho} \left\{ \frac{1}{a_{66}} - \left[a_{11} - \frac{(a_{13} + a_{44})^2}{a_{33} - a_{44}} \right]^{-1} \right\} \\
 &\quad \times \frac{1}{|z|} \delta\left(t - \frac{|z|}{\sqrt{a_{44}}}\right), \tag{6}
 \end{aligned}$$

$$G_{22}^{S(1)}(z, t) = -G_{11}^{S(1)}(z, t).$$

In eq. (6) we have used the basis of polarization vectors (4). Notice that the near-singularity term at the singularity behaves in the same way as the standard zeroth-order ray approximation: it has the same waveform and the same decrease of amplitude with distance from the source. That is why this term can be detected in the far field.

For the far-field ray-theory Green tensor at the singularity we obtain

$$\begin{aligned}
 G_{11}^{\text{far}}(z, t) &= G_{11}^{(0)}(z, t) + G_{11}^{S(1)}(z, t) \\
 &= \frac{1}{8\pi\rho} \left\{ \frac{1}{a_{66}} + \left[a_{11} - \frac{(a_{13} + a_{44})^2}{a_{33} - a_{44}} \right]^{-1} \right\} \\
 &\quad \times \frac{1}{|z|} \delta\left(t - \frac{|z|}{\sqrt{a_{44}}}\right), \\
 G_{22}^{\text{far}}(z, t) &= G_{22}^{(0)}(z, t) + G_{22}^{S(1)}(z, t) \\
 &= \frac{1}{8\pi\rho} \left\{ \frac{1}{a_{66}} + \left[a_{11} - \frac{(a_{13} + a_{44})^2}{a_{33} - a_{44}} \right]^{-1} \right\} \\
 &\quad \times \frac{1}{|z|} \delta\left(t - \frac{|z|}{\sqrt{a_{44}}}\right), \tag{7} \\
 G_{33}^{\text{far}}(z, t) &= G_{33}^{P(0)}(z, t) \\
 &= \frac{1}{4\pi\rho} \left[a_{44} + \frac{(a_{13} + a_{44})^2}{a_{33} - a_{44}} \right]^{-1} \frac{1}{|z|} \delta\left(t - \frac{|z|}{\sqrt{a_{33}}}\right).
 \end{aligned}$$

In contrast to formula (3), which describes the *S* wave in the far field incorrectly, formula (7) is correct for both *P* and *S* waves. The correctness of (7) at the singularity was verified by comparing this solution with the exact Payton analytical solution (Payton 1977; eqs 4.4–4.6). If we specify the Payton solution for the far field, we obtain an identical result. This implies that the near-singularity term is the only higher-order term of the ray expansion that is non-negligible in the far field. This applies to weak as well as strong transverse isotropy. It confirms the result of Vavryčuk & Yomogida (1996), who found that the Green tensor for the *SH* wave in TI media can be expressed exactly only by the zeroth- and the first-order ray approximations.

Comparing formulae (3) and (7) we find that the components of the far-field ray-theory Green tensor G_{11}^{far} and G_{22}^{far} can be simply expressed as an average of the components of the zeroth-order ray-theory Green tensor $G_{11}^{(0)}$ and $G_{22}^{(0)}$:

$$G_{11}^{\text{far}} = G_{22}^{\text{far}} = \frac{1}{2} [G_{11}^{(0)} + G_{22}^{(0)}]. \tag{8}$$

In (8) we assume that the kiss singularity is along the vertical axis. For a general orientation of the coordinate system, which is not connected to the singularity, formula (8) yields

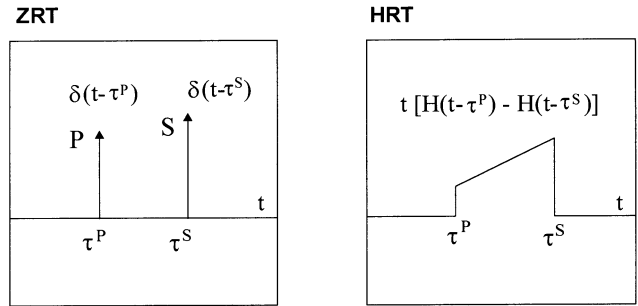
$$G_{kl}^{S \text{ far}}(\mathbf{x}, t) = \frac{1}{8\pi\rho} \frac{1}{v^S} \left(\frac{1}{\sqrt{K_p^{S1}}} + \frac{1}{\sqrt{K_p^{S2}}} \right) \frac{\delta_{kl} - g_k^p g_l^p}{r} \delta(t - \tau^S(\mathbf{x})), \tag{9}$$

where v^S is the group (or phase) velocity of the *S* wave in the singularity direction, τ^S is the travelttime of the *S* wave, $r = |\mathbf{x}|$ is the distance of the observation point from the source, \mathbf{g}^p is the unit polarization vector of the *P* wave orientated along the singularity direction, and K_p^{S1} and K_p^{S2} are the Gaussian curvatures of the *S1* and *S2* slowness surfaces at the singularity. The validity of this formula can be verified by comparing it with the asymptotic expansion of integral (1) at the kiss singularity (see Appendix, eq. A6).

2.5 Waves near a kiss singularity versus waves near a point source

The wavefield near a kiss singularity has many similarities to the wavefield near a point source (see Fig. 3). The similarities and differences between them can be summarized as follows (see Vavryčuk & Yomogida 1995; Vavryčuk 1997).

Wavefield near a point source



Wavefield near a kiss singularity

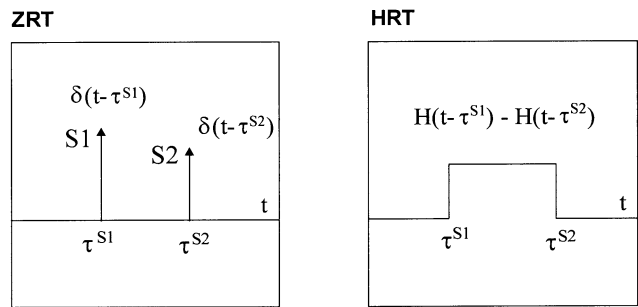


Figure 3. The Green's function in the near field in a homogeneous isotropic medium (upper plots) and the *S*-wave Green's function in the far field near a kiss singularity in a homogeneous TI medium (lower plots). The Green's functions are divided into parts described by the zeroth-order ray theory (ZRT, left-hand plots) and by the higher-order ray theory (HRT, right-hand plots).

(1) Neither wavefield is correctly described by the zeroth-order ray approximation, and hence higher-order ray approximations must be considered.

(2) In both wavefields, the higher-order ray approximations are non-zero at all times between the arrivals of the zeroth-order waves. Thus the higher-order ray approximations couple the zeroth-order waves.

(3) The amplitude of the near-field terms decreases with distance from the point source as $1/r^2$, and thus is negligible far from the source. The amplitude of the near-singularity term decreases with distance from the singularity as $1/R^2$, and thus is negligible far from the singularity.

(4) The near-singularity term can be significant in the near field as well as in the far field. In directions far from the singularity, it behaves like a near-field wave; in directions close to the singularity, it behaves like a far-field wave.

(5) The frequency content of the near-singularity and near-field terms depends on the separation times between the zeroth-order waves. For a small separation, the terms are of high frequency; for a large separation, the terms are of low frequency. At the singularity, the waveform of the near-singularity term is the Dirac delta function, and hence the near-singularity term and the zeroth-order waves have the same frequency content.

(6) The amplitude of the near-singularity term depends on the strength of anisotropy: for stronger anisotropy this term is more pronounced; in the limit from anisotropy to isotropy this term vanishes.

3 NUMERICAL MODELLING

In this section we demonstrate the properties of the near-singularity term (5) numerically. We consider *S* waves excited by a point source and propagating in a TI medium. We model the *S* waves by the zeroth-order ray approximation (when the near-singularity term is neglected) and by the far-field ray approximation (when the near-singularity term is considered). Both ray approximations will be compared with the exact solution calculated by computing formula (1) numerically. We use two models displaying TI: a medium with cracks and Mesaverde immature sandstone. The medium with cracks is assumed to be formed by an isotropic host rock with *P* and *S* velocities and density $\alpha = 4.50 \text{ km s}^{-1}$, $\beta = 2.53 \text{ km s}^{-1}$ and $\rho = 2.8 \text{ g cm}^{-3}$, respectively. The host rock contains aligned thin water-filled cracks with crack density $e = 0.1$ and aspect ratio $d = 0.001$. The resultant density-normalized elastic parameters of the cracked medium calculated using the Hudson model (Hudson 1981) are $a_{11} = a_{22} = 20.22$, $a_{33} = 20.04$, $a_{13} = 7.41$, $a_{44} = a_{55} = 5.10$ and $a_{66} = 6.38$. The anisotropy of the *P* wave is 3.5 per cent, and that of the *SV* and *SH* waves is 11.2 per cent (see Fig. 4). Shearer & Chapman (1989) use a similar cracked model (in their notation Model 1), but they use a different orientation of the symmetry axis and they also assume a non-zero velocity gradient. The second model, Mesaverde immature sandstone (Thomsen 1986), has the following elastic parameters: $a_{11} = a_{22} = 22.36$, $a_{33} = 18.91$,

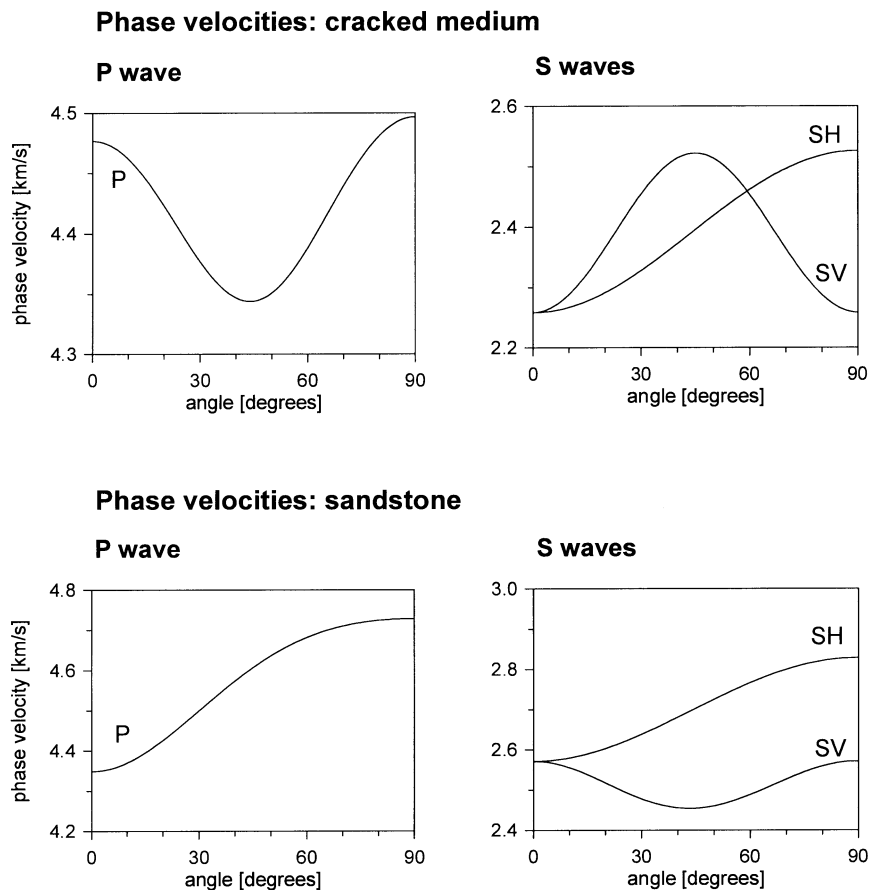


Figure 4. Phase velocities of the *P*, *SV* and *SH* waves as a function of the angle between the phase normal and the symmetry axis for the cracked medium and Mesaverde immature sandstone.

$a_{13} = 8.49$, $a_{44} = a_{55} = 6.61$, $a_{66} = 8.00$ and $\rho = 2.46 \text{ g cm}^{-3}$. The anisotropy of the P , SV and SH waves for this model reaches 8.3, 4.6 and 9.5 per cent, respectively (see Fig. 4).

The wavefield is generated by the single point force $\mathbf{F}(t) = \mathbf{F}f(t)$, where \mathbf{F} is the force vector, and $f(t)$ is the source-time function, which is defined as follows:

$$f(t) = \sin^2\left(\frac{\pi t}{T}\right) \text{ for } t \in \langle 0, T \rangle, \quad (10)$$

$$f(t) = 0 \text{ for } t \in (T, \infty),$$

where $T = 1 \text{ s}$. The parameter T specifies the width of the pulse. The source-time function generates waves in the form of a one-sided pulse in the far field. The force vector was chosen as $\mathbf{F} = (1, 1, 0)^T$.

Figs 5 and 6 display waveforms and particle motions of the S waves propagating in the cracked medium and in the sandstone. The waves are recorded at four observation points that lie in the x - z plane at distances from the source of $r = 225.8 \text{ km}$ for the cracked medium, and $r = 257.1 \text{ km}$ for the sandstone. This distance corresponds to 100 wavelengths of the S wave propagating in the direction of the symmetry axis of the medium. We used this very large distance to be sure that the far-field condition is well satisfied. The rays to the four observation points deviate from the symmetry axis by angles of $\vartheta = 2^\circ, 8^\circ, 14^\circ$ and 20° . Figs 5 and 6 show that the

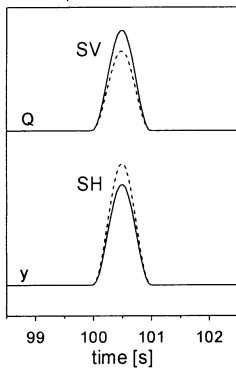
S waves separate in different ways at different observation points. As expected, almost no separation between the SV and SH waves is observed for the observation point closest to the singularity ($\vartheta = 2^\circ$). In contrast, at the point with $\vartheta = 20^\circ$, the SV and SH waves are fully separated in time in both media.

A comparison of the exact and ray solutions shows that the exact solution and the far-field ray solution coincide within the width of the line. This proves that the ray solution describes the S waves in the far field correctly, if the near-singularity term is considered. On comparing the far-field and the zeroth-order ray solutions, we conclude that the zeroth-order ray solution produces significant errors in amplitude as well as in polarization of the S waves, particularly in the vicinity of the singularity. We emphasize that both media under study can be considered as weakly anisotropic. For materials displaying stronger anisotropy, these errors can be even larger. Close to the singularity, the S waves do not separate, and the near-singularity term mainly affects the predominant polarization of the S wave. The fact that the actual predominant polarization of S waves can be remarkably different from the polarization predicted by the zeroth-order ray approximation has already been reported (but not explained) by Vavryčuk (1992; Fig. 13b). In the directions in which the S waves separate, the zeroth-order ray approximation predicts a linear polarization of the split S waves. If we consider the near-singularity term, the S -wave polarization is quasi-elliptical. For an increasing separation

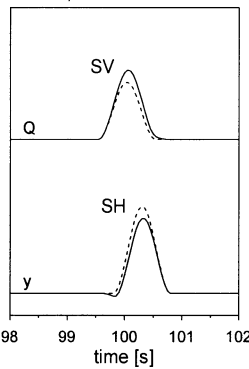
S waves near a kiss singularity (cracked medium)

Waveforms

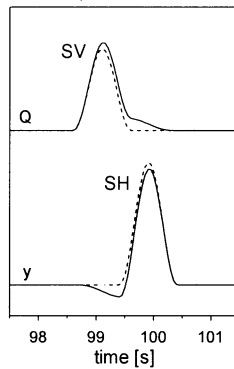
$\vartheta = 2^\circ, dt = 0.02 T$



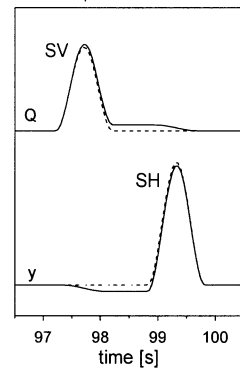
$\vartheta = 8^\circ, dt = 0.27 T$



$\vartheta = 14^\circ, dt = 0.81 T$

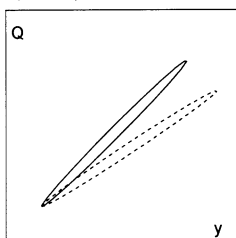


$\vartheta = 20^\circ, dt = 1.61 T$

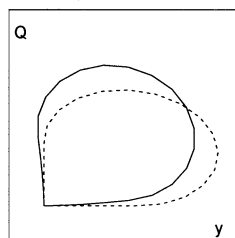


Particle motions

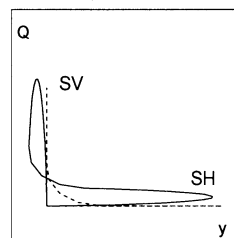
$\vartheta = 2^\circ, dt = 0.02 T$



$\vartheta = 8^\circ, dt = 0.27 T$



$\vartheta = 14^\circ, dt = 0.81 T$



$\vartheta = 20^\circ, dt = 1.61 T$

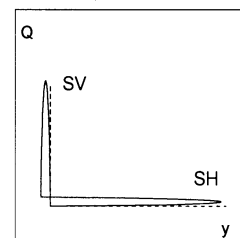
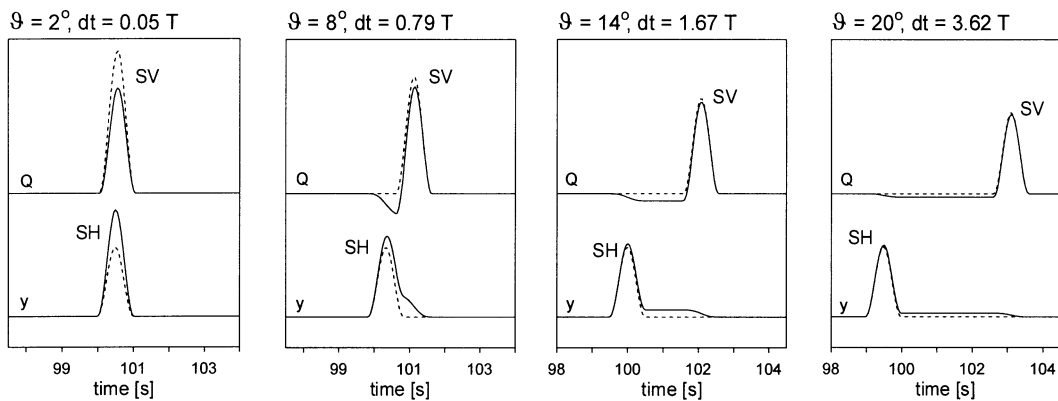


Figure 5. Waveforms and particle motions of S waves propagating in the cracked medium. Diagrams are shown for four receivers lying in the x - z plane at a distance $r = 225.8 \text{ km}$ from the source. Rays deviate from the kiss singularity by angles $\vartheta = 2^\circ, 8^\circ, 14^\circ$ and 20° . The parameter dt is the delay time between SV - and SH -wave arrivals, $T = 1 \text{ s}$ is the width of the pulse. Component Q lies in the x - z plane and is perpendicular to the ray. Dashed line: zeroth-order ray solution; full line: exact solution and/or far-field ray solution.

S waves near a kiss singularity (sandstone)

Waveforms



Particle motions

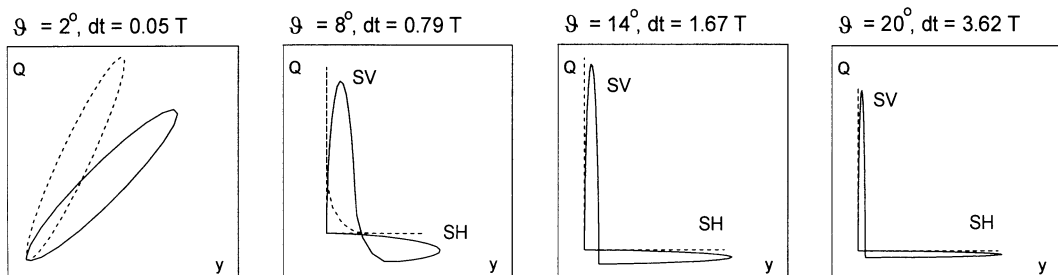


Figure 6. Waveforms and particle motions of S waves propagating in Mesaverde immature sandstone. Receivers lie at a distance $r = 257.1$ km from the source. Dashed line: zeroth-order ray solution; full line: exact solution and/or far-field ray solution.

time between the split S waves, the quasi-ellipticity decreases. In directions far from the singularity, the quasi-ellipticity is negligible, and thus the S waves are successfully reproduced by the zeroth-order ray approximation.

4 CONCLUSIONS

We have studied the exact solution and the approximate ray solutions of S waves generated by a point source in a homogeneous, transversely isotropic, elastic medium and propagating in directions close to a kiss singularity. We have proved that it is possible to construct a ray solution that can correctly describe the S waves far from the source in all directions, including that of the kiss singularity. We have proved this analytically by comparing the ray solution with the exact analytical Payton solution (Payton 1977, 1983), and by comparing the ray solution with the far-field solution at the kiss singularity (see Appendix). We have also proved this numerically by comparing the ray solution with the numerically evaluated exact integral solution (Burrige 1967; Wang & Achenbach 1994).

We found that in directions far from the kiss singularity, the S waves are reproduced satisfactorily by the zeroth-order ray approximation. In directions near the kiss singularity, the zeroth-order ray approximation yields distorted results. In these directions, the first-order ray approximation is significant,

and must be considered. We therefore call this first-order term of the ray expansion the near-singularity term. *The near-singularity term can be of high frequency and it can be detected in the far field.* At the singularity, this term has the same waveform and the same frequency content as the zeroth-order ray approximation. The amplitude of the near-singularity term decreases in the same way as the zeroth-order term. The near-singularity term appears at the times between the arrivals of the split zeroth-order S waves, causing the S waves to become coupled. This coupling is in many aspects similar to the coupling of the P and S waves near a point source. If the zeroth-order S waves are not well separated, forming only one S wave, the near-singularity term can change the predominant direction of the S -wave polarization. If the zeroth-order S waves are separated in time, then the near-singularity term can cause both S waves to be quasi-elliptically polarized. The quasi-ellipticity of the split S waves decreases with increasing separation time. The amplitude of the near-singularity term depends on the strength of anisotropy: for isotropic media this term vanishes. With the aid of numerical examples we have shown that the near-singularity term can strongly affect the S waves propagating in weakly anisotropic TI media, a common scenario in crustal seismology. It can affect the polarization of the S waves propagating in directions up to 15° from the kiss singularity, and at distances of up to hundreds of wavelengths from the source.

ACKNOWLEDGMENTS

I thank V. Červený and I. Pšenčík for critically reading the manuscript and offering their comments. I thank Dr Colin Thomson for a very helpful and stimulating review. The work was supported by the Grant Agency of the Czech Republic, Grant no. 205/96/0968, by the Consortium Project 'Seismic waves in complex 3-D structures' and by the EC INCO-Copernicus Project IC15 CT96 200.

REFERENCES

- Buchwald, V.T., 1959. Elastic waves in anisotropic media, *Proc. R. Soc. Lond. A*, **253**, 563–580.
- Burridge, R., 1967. The singularity on the plane lids of the wave surface of elastic media with cubic symmetry, *Q. J. Mech. appl. Math.*, **20**, 41–56.
- Červený, V., 1972. Seismic rays and ray intensities in inhomogeneous anisotropic media, *Geophys. J. R. astr. Soc.*, **29**, 1–13.
- Červený, V., Molotkov, I.A. & Pšenčík, I., 1977. *Ray Method in Seismology*, Charles University Press, Praha.
- Crampin, S., 1991. Effects of point singularities on shear-wave propagation in sedimentary basins, *Geophys. J. Int.*, **107**, 531–543.
- Crampin, S. & Yedlin, M., 1981. Shear-wave singularities of wave propagation in anisotropic media, *J. Geophys.*, **49**, 43–46.
- Hudson, J.A., 1981. Wave speeds and attenuation of elastic waves in material containing cracks, *Geophys. J. R. astr. Soc.*, **64**, 133–150.
- Kendall, J.-M., Guest, W.S. & Thomson, C.J., 1992. Ray-theory Green's function reciprocity and ray-centred coordinates in anisotropic media, *Geophys. J. Int.*, **108**, 364–371.
- Lighthill, M.J., 1960. Studies on magneto-hydrodynamic waves and other anisotropic wave motions, *Phil. Trans. R. Soc. Lond., A*, **252**, 397–430.
- Mura, T., 1991. *Micromechanics of Defects in Solids*, Kluwer Academic Publishers, London.
- Payton, R.G., 1977. Symmetry-axis elastic waves for transversely isotropic media, *Q. appl. Math.*, **35**, 63–73.
- Payton, R.G., 1983. *Elastic Wave Propagation in Transversely Isotropic Media*, Martinus Nijhoff Publishers, The Hague.
- Rümpker, G. & Thomson, C.J., 1994. Seismic-waveform effects of conical points in gradually varying anisotropic media, *Geophys. J. Int.*, **118**, 759–780.
- Shearer, P.M. & Chapman, C.H., 1989. Ray tracing in azimuthally anisotropic media—I. Results for models of aligned cracks in the upper crust, *Geophys. J.*, **96**, 51–64.
- Thomsen, L., 1986. Weak elastic anisotropy, *Geophysics*, **51**, 1954–1966.
- Vavryčuk, V., 1992. Polarization properties of near-field waves in homogeneous isotropic and anisotropic media: numerical modelling, *Geophys. J. Int.*, **110**, 180–190.
- Vavryčuk, V., 1997. Elastodynamic and elastostatic Green tensors for homogeneous weak transversely isotropic media, *Geophys. J. Int.*, **130**, 786–800.
- Vavryčuk, V. & Yomogida, K., 1995. Multipolar elastic fields in homogeneous isotropic media by higher-order ray approximations, *Geophys. J. Int.*, **121**, 925–932.
- Vavryčuk, V. & Yomogida, K., 1996. SH-wave Green tensor for homogeneous transversely isotropic media by higher-order approximations in asymptotic ray theory, *Wave Motion*, **23**, 83–93.
- Wang, C.-Y. & Achenbach, J.D., 1994. Elastodynamic fundamental solutions for anisotropic solids, *Geophys. J. Int.*, **118**, 384–392.

APPENDIX A: FAR-FIELD S-WAVE GREEN TENSOR AT THE KISS SINGULARITY IN TI MEDIA

Following Burridge (1967; eq. 6.7) we can express the asymptotic formula of the Green tensor $G_{kl}^{S \text{ far}}(\mathbf{x}, t)$ in the following form:

$$G_{kl}^{S \text{ far}}(\mathbf{x}, t) = -\frac{H(t)}{8\pi^2 \rho} \sum_{m=1}^2 \int_{S^e} F_{kl}^m(\mathbf{p}) \times \delta \left(t - \mathbf{p}_0 \cdot \mathbf{x} + \frac{1}{2} K_{11}^m |\mathbf{x}| p_1^2 + \frac{1}{2} K_{22}^m |\mathbf{x}| p_2^2 \right) dp_1 dp_2, \quad (\text{A1})$$

$$F_{kl}^m(\mathbf{p}) = \frac{g_k^m g_l^m}{v^m},$$

where the superscript $m = 1, 2$ denotes the S1 and S2 waves, K_{11} and K_{22} are the principal curvatures of the slowness surface at stationary point \mathbf{p}_0 , v is the group velocity, and \mathbf{x} is the position vector of the observation point. Local coordinates p_1 and p_2 have their origin at \mathbf{p}_0 , and are parallel to lines of the principal curvature at \mathbf{p}_0 . The integration is over the small neighbourhood S^e of point \mathbf{p}_0 of slowness surface S .

Let us consider a TI medium with a kiss singularity parallel to the p_3 -axis. The superscript $m = 1, 2$ then denotes the SV and SH waves, principal curvatures K_{11}^m and K_{22}^m are equal, and amplitude $F_{kl}^m(\mathbf{p})$ reads

$$F_{kl}^{SV}(\vartheta, \varphi) = \frac{1}{v^{SV}(\vartheta)} \times \begin{bmatrix} \cos^2 \varphi \cos^2 \vartheta & \sin \varphi \cos \varphi \cos^2 \vartheta & -\cos \varphi \sin \vartheta \cos \vartheta \\ \sin \varphi \cos \varphi \cos^2 \vartheta & \sin^2 \varphi \cos^2 \vartheta & -\sin \varphi \sin \vartheta \cos \vartheta \\ -\cos \varphi \sin \vartheta \cos \vartheta & -\sin \varphi \sin \vartheta \cos \vartheta & \sin^2 \vartheta \end{bmatrix},$$

$$F_{kl}^{SH}(\vartheta, \varphi) = \frac{1}{v^{SH}(\vartheta)} \begin{bmatrix} \sin^2 \varphi & -\sin \varphi \cos \varphi & 0 \\ -\sin \varphi \cos \varphi & \cos^2 \varphi & 0 \\ 0 & 0 & 0 \end{bmatrix}, \quad (\text{A2})$$

where ϑ denotes the angle between singularity direction \mathbf{p}_0 and slowness vector \mathbf{p} , and φ denotes the azimuth of \mathbf{p} in the p_1 - p_2 plane. Obviously, functions $F_{kl}^{SV}(\vartheta, \varphi)$ and $F_{kl}^{SH}(\vartheta, \varphi)$ are not continuous at the singularity ($\vartheta = 0$). This implies that eq. (6.8) of Burridge (1967) cannot be applied as it is, but needs to be modified. Expressing integral (A1) in spherical coordinates, we obtain

$$G_{kl}^{S \text{ far}}(\mathbf{x}, t) = -\frac{H(t)}{8\pi^2 \rho} \sum_{m=1}^2 \int_{S^e} F_{kl}^m(\vartheta, \varphi) \times \delta \left(t - \mathbf{p}_0 \cdot \mathbf{x} + \frac{1}{2} \sqrt{K_p^m} |\mathbf{x}| p^2 \sin^2 \vartheta \right) p^2 \sin \vartheta d\vartheta d\varphi, \quad (\text{A3})$$

where K_p is the Gaussian curvature of the slowness surface at the singularity, and $p = p(\vartheta)$ is the magnitude of the slowness vector. Taking into account that

$$\int_0^{2\pi} F_{kl}^{SV}(\vartheta, \varphi) d\varphi = \frac{\pi}{v^{SV}(\vartheta)} \begin{bmatrix} \cos^2 \vartheta & 0 & 0 \\ 0 & \cos^2 \vartheta & 0 \\ 0 & 0 & 2 \sin^2 \vartheta \end{bmatrix}, \tag{A4}$$

$$\int_0^{2\pi} F_{kl}^{SH}(\vartheta, \varphi) d\varphi = \frac{\pi}{v^{SH}(\vartheta)} \begin{bmatrix} 1 & 0 & 0 \\ 0 & 1 & 0 \\ 0 & 0 & 0 \end{bmatrix},$$

we can integrate (A3) over φ and ϑ , and calculate the result for vanishing ϑ . We then obtain

$$G_{kl}^{S \text{ far}}(\mathbf{x}, t) = \frac{1}{8\pi\rho} \frac{1}{v^S} \left(\frac{1}{\sqrt{K_p^{SV}}} + \frac{1}{\sqrt{K_p^{SH}}} \right) \frac{A_{kl}}{|\mathbf{x}|} \delta(t - \mathbf{p}_0 \cdot \mathbf{x}),$$

where

$$A_{kl} = \begin{bmatrix} 1 & 0 & 0 \\ 0 & 1 & 0 \\ 0 & 0 & 0 \end{bmatrix}. \tag{A5}$$

In (A5) we use the local coordinate system with the x_3 -axis along the singularity. In a general coordinate system, formula (A5) yields

$$G_{kl}^{S \text{ far}}(\mathbf{x}, t) = \frac{1}{8\pi\rho} \frac{1}{v^S} \left(\frac{1}{\sqrt{K_p^{S1}}} + \frac{1}{\sqrt{K_p^{S2}}} \right) \frac{\delta_{kl} - g_k^P g_l^P}{|\mathbf{x}|} \delta(t - \mathbf{p}_0 \cdot \mathbf{x}), \tag{A6}$$

where v^S is the group (or phase) velocity of the S wave at the singularity, \mathbf{g}^P is the unit polarization vector of the P wave orientated along the singularity, and K_p^{S1} and K_p^{S2} are the Gaussian curvatures of the S1 and S2 slowness surfaces at the singularity.